Improvement of CO_2/N_2 separation performance by polymer matrix cellulose acetate butyrate

R J Lee[1], Z A Jawad[1]*, A L Ahmad[2], J Q Ngo[1], H B Chua[1]

[1] School of Engineering and Science, Department of Chemical Engineering, Curtin University Sarawak Malaysia, CDT 250, Miri 98009, Sarawak, Malaysia
[2] School of Chemical Engineering, Engineering Campus, Universities Sains Malaysia, 14300 Nibong Tebal, Penang, Malaysia

E-mail: zeinab.aj@curtin.edu.my

Abstract. With the rapid development of modern civilization, carbon dioxide (CO_2) is produced in large quantities and mainly generated from industrial sectors. The gas emission is the major contributor to global warming. To address this issue, the membrane technology is implemented for the CO_2 removal, due to the energy efficiency and economic advantages presented. Cellulose acetate butyrate (CAB) is selected as the polymeric material, due to the excellent film-forming properties and capable of developing a defect-free layer of neat membrane. This study described the fabrication development of CAB using a wet phase inversion method with different casting conditions. Where the composition of the casting solutions (3-5 wt %) and solvent evaporation time (4-6 min) were determined. The outcomes of these dominant parameters were then used to determine the best CAB membrane for CO_2/Nitrogen (N_2) separation and supported by the characterization i.e. scanning electron micrograph. Gas permeation measurements showed satisfactory performance for CAB membrane fabricated with 5 min evaporation time and 4 wt% polymer composition (M2). Where, its permeance and selectivity are 120.19 GPU and 3.17, respectively. In summary, this study showed a brief outlined of the future direction and perspective of CAB membrane for CO_2/N_2 separation.

1. Introduction

In the past century, carbon dioxide (CO_2) is widely known as the leading contributor to global warming. A total of 35.4 billion tonnes of CO_2 was emitted to the environment annually [1]. With the rising of the greenhouse gasses (GHGs) effect, which increases the atmospheric concentration of CO_2, this had caused lots of concern amongst the researchers in combating this global issue. CO_2 is being classified as the most significant anthropogenic GHGs and partaking around two-third of the GHGs composition [2-4]. The primary source of CO_2 emission is commonly found in the natural gas streams, biogas, and flue gas from fossil fuel combustion [5].

Due to the enormous amount of CO_2 emission back in the mid-19th century, the application of membrane technology had increased remarkably since the first invention in 1981 [6]. The membrane gas separation technology is designed with the purpose to separate individual gas component based on the different permeation rates of each gas component through a thin membrane barrier [7]. The membrane separation performance characteristics are commonly indicated by permeation and selectivity [8]. In an ideal situation, high permeability is preferable while maintaining high selectivity, therefore smaller membrane area and lower driving force is required. Thus, such ideal conditions require less operating cost and hence lower capital cost [9, 10].

There are less than ten types of polymer materials that have been used for at least 90% of the total installed membrane-based gas separation modules, including cellulose acetate butyrate (CAB), cellulose acetate (CA), polyimide, polyamide, polysulfone, polycarbonates, polyethersulfone, and polyphenylene oxide [11]. Based on Basu, Khan [12], the CAB exhibits excellent film-forming properties, the butyryl group in CAB can effectively improve and expand the capacity of the material volume cellulose chain membrane through enlarging the free volume [12]. CAB polymer possess several prominent characteristics including high impact resistance, well-maintained weather resistance, notable chemical resistance with excellent film forming characteristics inherited from acetyl and butyl groups [13].

However, polymeric membrane formation usually involved a series of complex process which depends on a vast variety of parameters [14] such as polymer concentration, and solvent evaporation time [15]. In this regard, Jansen, Macchione [14] proved that the solvent evaporation duration is relatively necessary to determine the membrane gas diffusion and solubility coefficients through sorption measurement [14]. Paulsen, Shojaie [16] investigated the effects of duration of the evaporation step between 10-150 s. They found out that increasing the length of solvent evaporation always tend to damp macro voids formation for CA membrane. The reduction of the microvoids formation eventually improved the overall selectivity of the CA membrane [16]. Also, the polymer concentration plays a key factor in the membrane formation. Where increasing the polymer concentration reduced the microvoids of the membrane due to dense skin formation [17]. The increase in polymer concentration also improved the selectivity performance of the membrane, due to the tighter structural membrane formed [18].

Thus, the aim of the present work is to improve the separation performance of CAB membrane towards CO_2/N_2 by investigating the effect of solvent evaporation time (chloroform) and CAB polymer concentration. Up to date, there is no report has examined this parameter yet. Whereby, both studied dominant parameters will then utilized in the fabrication of mixed matrix membrane (MMM).

2. Methodologies

2.1. Materials

CAB polymer (70,000 Mn) with an acetyl group (12%-15%) was purchased from Sigma-Aldrich (Malaysia). The chemical solutions required for the membrane fabrication were chloroform, isopropyl alcohol (99.6%) and n-hexane (99.8%), which can purchase from Merck (Malaysia).

2.2. CAB membrane preparation

The CAB membrane was fabricated using the phase inversion method. The solution consists of 4 wt% CAB and 96 wt% chloroform, was stirred for 24 hrs [19]. Then, the dope solution was sonicated for 20 min to eliminate the bubble in solution to ensure the surface homogenous of the neat membrane [19]. The dope solution was cast using the automatic film applicator on a glass plate, under the standard operating fume hood. A uniform casting thickness of 250 μm was applied. Allow 5 min solvent evaporation time to evaporate the solvent followed by immersing the membrane film in distilled water (0-22 °C) for 24 hr [20]. The as-spun membrane was immersed in isopropyl alcohol for 1 hr followed by n-hexane for another 1 hr [20]. The resultant membrane (M1) was dry in the oven at 70 °C to eliminate the remaining volatile liquid between two glass plates for 24 hr and stored before use [20].

2.2.1. Effect of solvent evaporation time. The solution was cast based on the synthesis method described in section 2.2. The studied range was from 4 min to 6 min. The composition of the membrane fabrication process is shown in table 1.

Table 1. The composition of membrane prepared at different solvent evaporation time

Sample Description	CAB (wt%)	Chloroform (wt%)	Casting Thickness (μm)	Evaporation time (min)
M1	4	96	250	4
M2	4	96	250	5
M3	4	96	250	6

2.2.2. Effect of CAB polymer concentration. The solution was cast based on the synthesis method described in section 2.2. The studied range was from 3 wt% to 5 wt%. The composition of the membrane fabrication process is shown in table 2.

Table 2. The composition of membrane prepared at different CAB polymer concentration

Sample Description	CAB (wt%)	Chloroform (wt%)	Casting Thickness (μm)	Evaporation time (min)
M4	3	97	250	5
M2	4	96	250	5
M5	5	95	250	5

2.3. Membrane characterization

2.3.1. Scanning electron microscopy (SEM). The membrane surface morphology and cross-section were observed with a scanning electron microscope (Hitachi TM3000, Tokyo, Japan). Each membrane sample was cut into small pieces and was kept in the cryogenic freezer with plastic petri dish up to -80 °C for 24 hr to give a consistent and clean cut by freezing. The samples were then coated with platinum to prevent the accumulation of static charges at the specimen. Also, the membrane thickness of every sample was calculated based on the frequency count that was observed in these images using Image J software. Approximately 100 measurements were taken to confirm it.

2.4. Gas permeability measurement

Single gas permeation tests were conducted using either pure N_2 or CO_2 gas at room temperature. The kinetic diameter of the N_2 and CO_2 were 3.64 $\dot{A}$ and 3.3 $\dot{A}$, respectively. The schematic diagram of the experimental rig shows in figure 1. For each single gas permeation test, the flow rate of the gas was controlled at 100 ml/min using the mass flow controller (Aalborg AFC26, USA) and gas supplied from compressed gas cylinder tank.

The mass flow controller was connected to a two-channel digital set point/ readout unit (Aalborg 0-200 ml/min, USA). The feed gas pressure for each of the gasses was set from 1-2 bars throughout the experimental investigation. Prior the experiment, leak detection test was conducted to ensure no feed gas escape from the rig pipes. Allowed the feed N_2 gas to flow throughout the rig for 10 min, to purge out the impurities gas inside the pipe. After that, the fabricated membrane was cut into a round disc shape with an effective diameter of 7.065 cm^2 and placed in the membrane permeation cell. Covered and tightened the membrane permeation cell before connecting it back to the streams. The permeate flow rate can be obtained and measured through the volume displacement of the soap bubble flow meters.

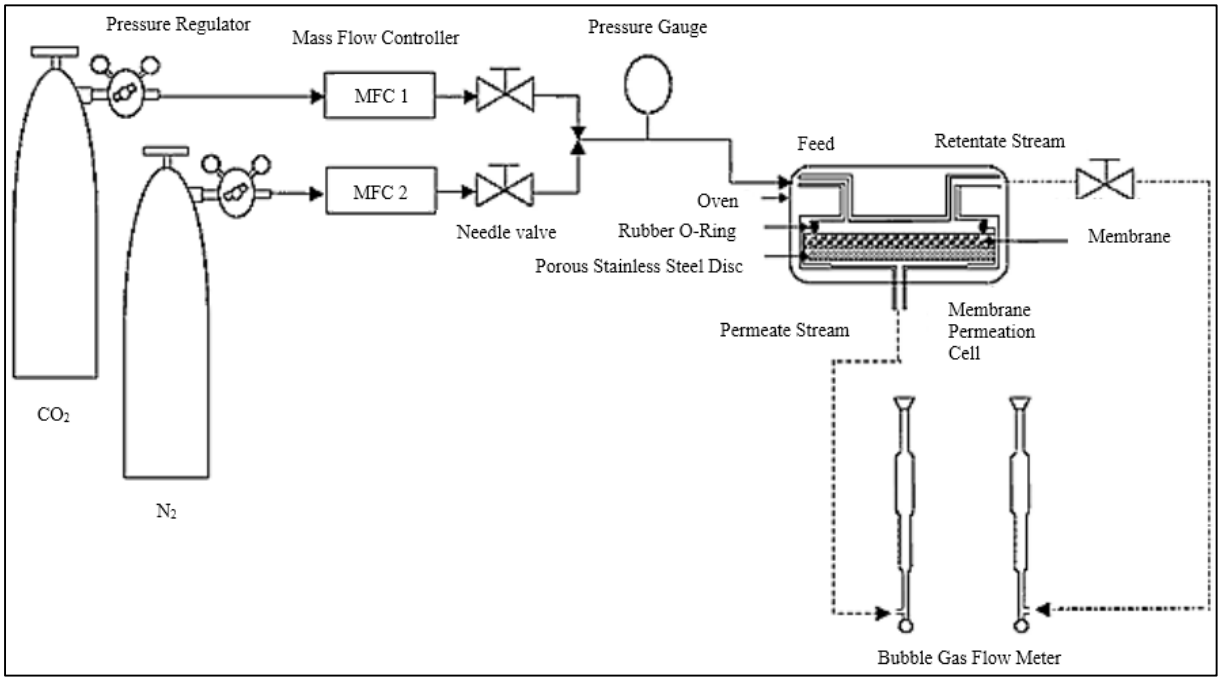

Figure 1. Schematic Diagram of the Experimental Rig

The permeance of the membrane is indicated by (P/ℓ), which can be calculated using equation (1) and the unit of the permeance was expressed in GPU. Whereby the l represent the membrane thickness in cm, Q the volumetric flow rate indicated from flow meter in cm^3/s, A is the effective membrane area in cm^2, and ΔP is the pressure difference in the membrane permeation cell which is expressed in cmHg [22].

$$(P/\ell) = (Q/A\Delta P) \quad (1)$$

Meanwhile, the selectivity of the membrane can be determined using the ideal separation factor (α) as shown in equation (2) [22].

$$\alpha_{CO_2/N_2} = P_{CO_2}/P_{N_2} = [(P/l)_{CO_2}/(P/l)_{N_2}] \quad (2)$$

Whereby, the P_{CO_2} and P_{N_2} represent the permeability of components CO_2 and N_2, respectively [23]. Each membrane specimens were tested at least 4 times to ensure precision of the results generated. The average values together with the standard errors, were reported.

3. Results and discussion

3.1. Effect of solvent evaporation duration

The solvent evaporation period is one of the crucial parameters that manipulates the membrane morphology. SEM was utilized to observe the physical morphology of the CAB, as shown in figure 2. The figure 2a and figure 2c shown smooth surface for M1 with evaporation time of 4 min and M2 with evaporation time of 5 min. On the other hand, the M3 membrane with evaporation time of 6 min is undergoing a transitional phase from smooth surface to porous surface structure. Provided with longer evaporation time, rapid diffusion of the solvent (chloroform) can occur, where the chloroform evaporated from the as-spun membrane before the water immersion [24]. Thus, porous and dense structures were formed.

According to figure 2, M1 (4 min), M2 (5 min), and M3 (6 min) show a thickness of 497.8 µm, 148.2 µm, and 555.7 µm, respectively. This was due to the compact properties of CAB chains in the formation of M2 membrane during the controlled solvent evaporation period (5 min), forming a thin membrane [29]. However, M3 membrane shows thicker membrane of 555.7 µm. This was due to the rapid evaporation of the casting solvent from the membrane due to prolonged evaporation time (6 min), hence causing an expansion in the membrane volume. Moreover, the thicker membrane exerts more flow resistance to the membrane, which typically yields a low separation performance membrane [16, 29].

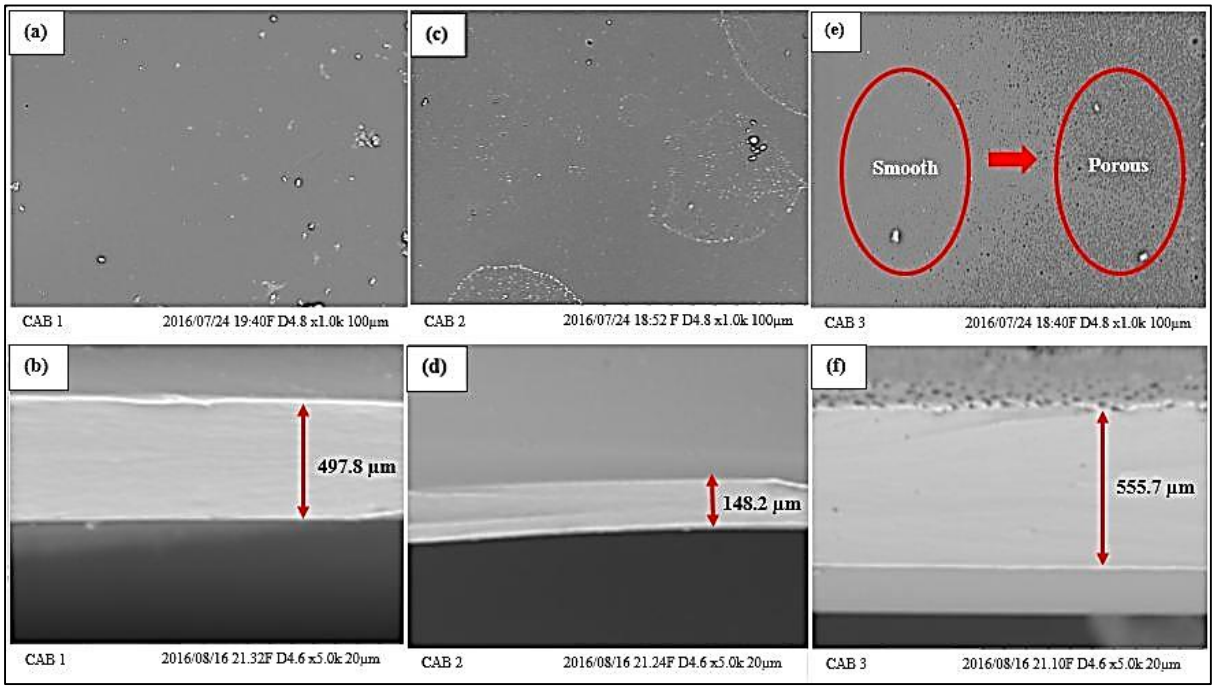

Figure 2. SEM morphologies of surface and cross section of CAB membrane with evaporation time of (a-b) 4 min (M1), (c-d) 5 min (M2), and (e-f) 6 min **(**M3)

According to table 3, M3 with the longest solvent evaporation time up to 6 min yield highest permeance results ranging from 1005-1253 GPU as compared to M1 (107-117 GPU) and M2 (37-120 GPU). This can explain by the arising porous surface structure exhibited in M3 (figure 2e). It was due to prolong the evaporation period of the highly volatile solvent (chloroform), causing a high volume of solvent evaporation outflow during solvent evaporation period [25]. It might allow the gas to escape through the membrane structure quickly. However, the selectivity is significantly reduced due to the high permeance rate causing the trade-off relationship between permeance and selectivity performance. On the other hand, consistent permeance results were observed for both M1 and M2 membranes, and M2 membrane with 5 min solvent evaporation time is preferable due to the better selectivity was shown.

Table 3. Permeability and selectivity performance for M1, M2, and M3

	M1			**M2**			**M3**		
Pressure (Bar)	**P_{CO2} (GPU)**	**P_{N2} (GPU)**	**α**	**P_{CO2} (GPU)**	**P_{N2} (GPU)**	**α**	**P_{CO2} (GPU)**	**P_{N2} (GPU)**	**α**
1.0	113.06	116.03	0.97	40.51	119.20	2.94	1010.74	1253.49	1.24
1.5	117.84	107.49	1.10	37.83	116.91	3.09	1005.34	1251.43	1.25
2.0	111.79	109.33	1.02	37.91	120.19	3.17	1006.46	1253.71	1.25

Meanwhile, M2 shows higher CO_2/N_2 separation performance with a selectivity of 2.94-3.17 as compared to M1 (0.97-1.02) and M3 (1.24-1.25) in figure 3. This proved that the CAB membrane

achieved the highest selectivity of CO_2 with 6 min solvent evaporation time, due to the smooth surface layer which selectively allows a predetermine amount of CO_2 to pass through the dense membrane which was supported with the solution-diffusion mechanism [26].

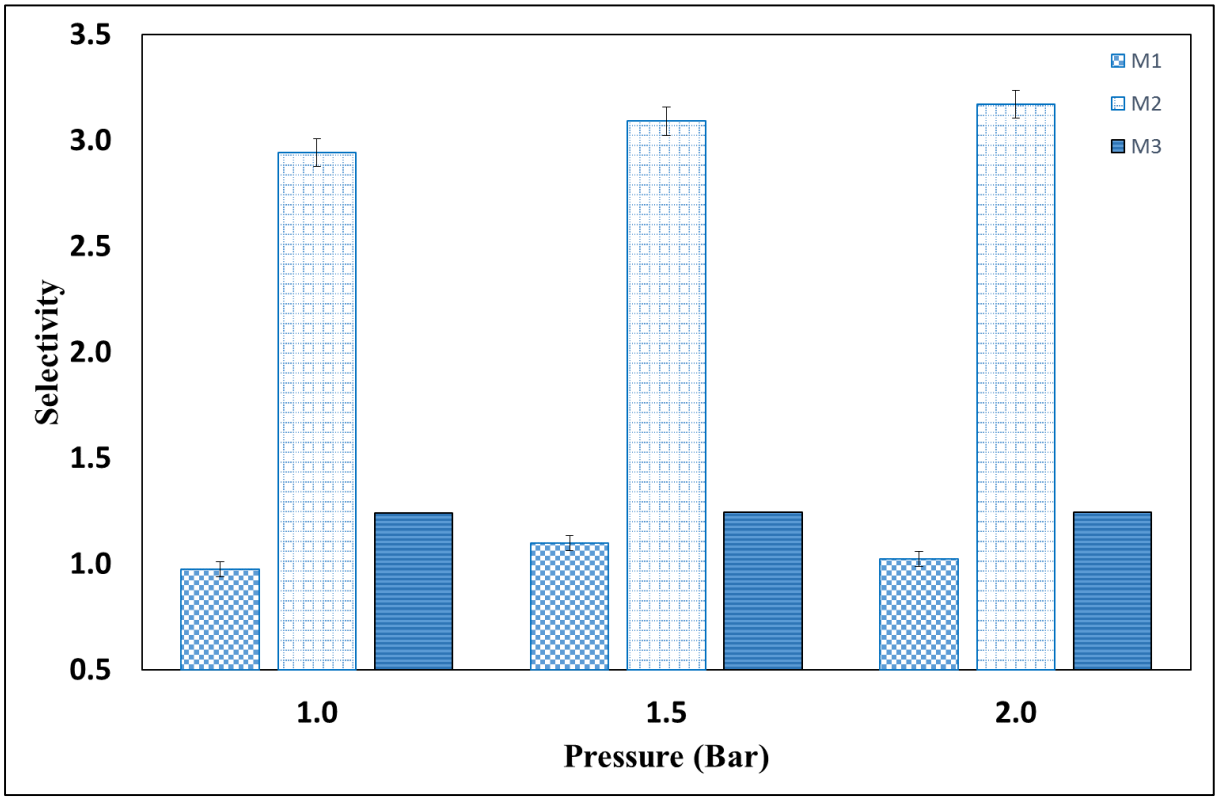

Figure 3. Ideal selectivity of CO_2/N_2 through CAB membrane with evaporation time of 4 min (M1), 5 min (M2), and 6 min **(**M3).

3.2. Effect of polymer concentration

The polymer loading concentration is another dominant factor that affects the surface morphology of the membrane. Figure 4 demonstrates the top surface and cross-sectional morphology at polymer concentrations of 3 wt% (M4), 4 wt% (M2), and 5 wt% (M5). A porous surface membrane structure was observed for M4 **(**figure 4a) at 3 wt% of CAB polymer. However, the CAB membrane morphology changes from porous to smooth dense membrane when the polymer concentration increases to 4 wt% (M2) and 5 wt%, as shown in figure 4c and 4e, respectively. This can be explained with the increment in the viscosity of the polymer, hence reducing the fluid of solution, thus causes the delayed demixing in the coagulant bath [18].

Based on table 4, M4 yield highest permeance results ranging from 303-318 GPU as compared to M2 (37-98 GPU) and M5 (50-98 GPU). The possible explanation for M4 membrane having high permeance rate is due to the porous surface layer which allows the gas to escape through a less resistance pathway. As compared to M2 with a thickness of 148.2 µm, M4 and M5 membranes have a thicker membrane of 355.2 µm and 441.2 µm, respectively, as demonstrated in figure 2b and figure 2f. This was due to the effect of a smaller concentration gradient, compensated by a much lower casting solution viscosity [27]. On the other hand, the membrane M4 supposedly should exhibit thin dense membrane. However due to the high solvent composition with low polymer concentration (3 wt%), more solvent evaporated from the membrane resulting in an increase in membrane thickness to 355.2 µm (Asgarkhani et al. 2013). This thicker membrane reduced the separation results of the membranes. Thus, it proved

that the effect of the membrane thickness is to exert additional flow resistance to the membrane, therefore less effective membrane yield (Lan et al. 2005).

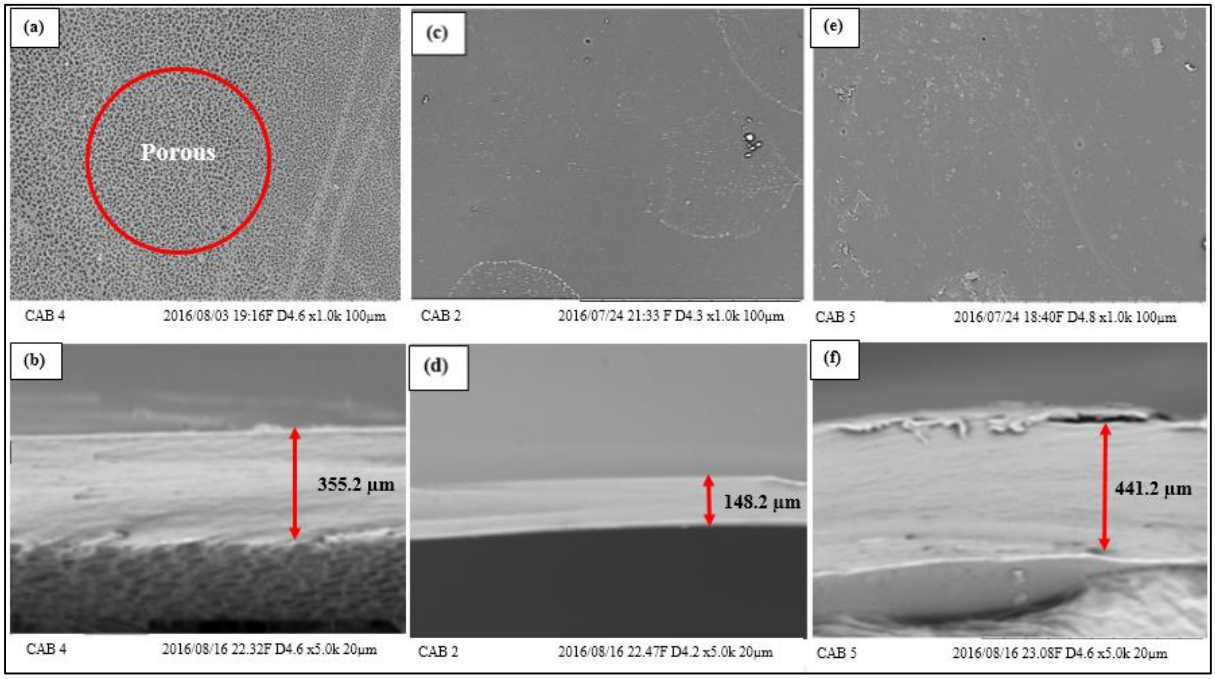

Figure 4. SEM morphologies of surface and cross section of CAB membrane with a polymer concentration of (a-b) 3 wt% (M4), (c-d) 4 wt% (M2), and (e-f) 5 wt% **(**M5).

The ideal selectivity of M2, M4 and M5 was also investigated as shown in figure 5. The M2 membrane proved to have the best selectivity results amongst the others (M4 and M5). The possible explanation was when low polymer concentration was substituted, the morphology of membrane became less compact with big aperture, resulting in the high flux of membrane while decreasing the diffusion selectivity [27]. Moreover, this causes the structure of membrane become more compact, resulting in less flux, and thus lower the diffusion selectivity [28]. In summary, the M2 membrane with 4 wt% of CAB polymer has the best CO_2/N_2 separation performance.

Table 4. Permeability and selectivity performance for M2, M4, and M5

	M4			M2			M5		
Pressure (Bar)	**P_{CO2} (GPU)**	**P_{N2} (GPU)**	**α**	**P_{CO2} (GPU)**	**P_{N2} (GPU)**	**α**	**P_{CO2} (GPU)**	**P_{N2} (GPU)**	**α**
1.0	317.94	303.43	1.05	40.51	119.20	2.94	98.11	50.28	1.95
1.5	313.05	306.68	1.02	37.83	116.91	3.09	93.63	50.49	1.85
2.0	318.95	304.48	1.05	37.91	120.19	3.17	90.75	50.57	1.79

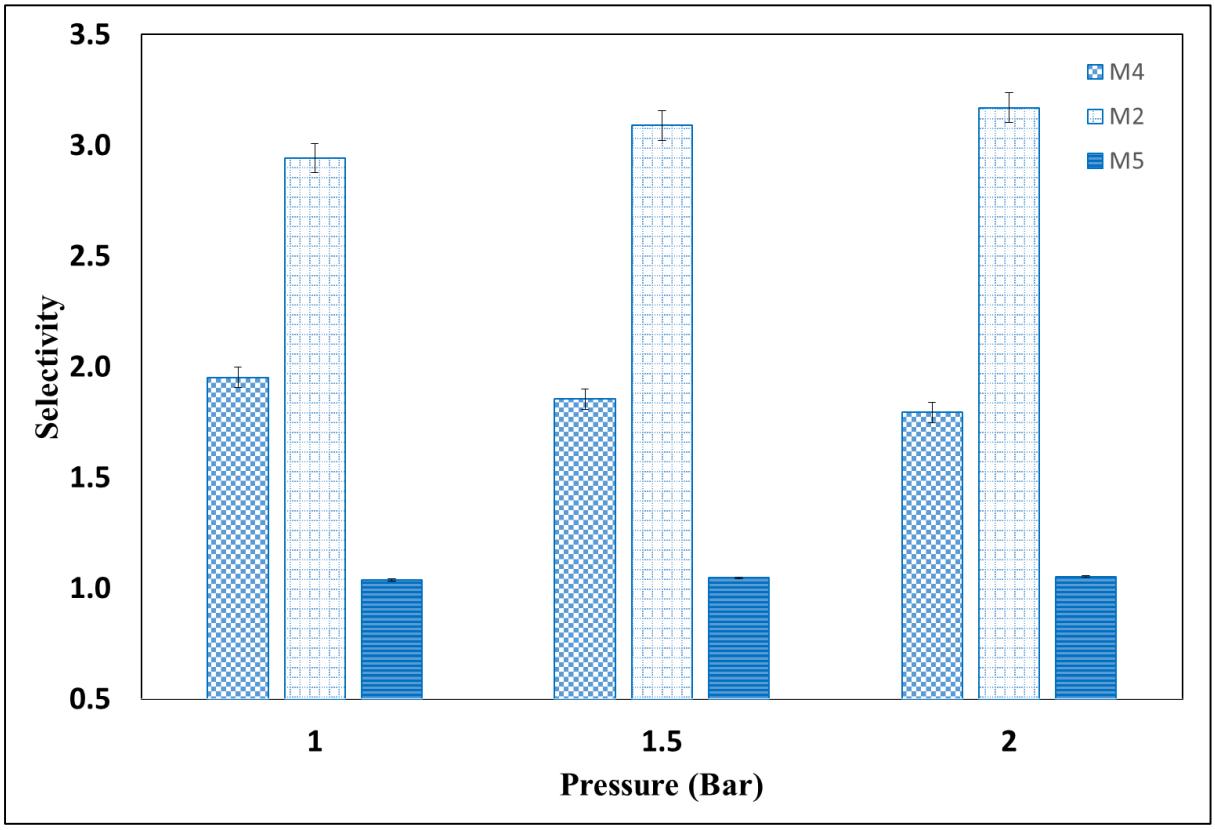

Figure 5. Ideal selectivity of CO_2/N_2 through CAB membrane with polymer concentration 3 wt% (M4), 4 wt% (M2), and 5 wt% **(**M5).

4. Conclusion

In the present work, it was found that the solvent evaporation duration and concentration of the polymer correlate closely in manipulating the membrane morphology and ultimately affect the CO_2/N_2 separation performance of CAB membrane. The dominant parameters for solvent evaporation time and CAB polymer concentration were 5 min with 4 wt% concentration loading which was represented by M2. Meanwhile, to improve the CO_2/N_2 selectivity of the CAB membrane, it was suggested to incorporate the CAB polymer with inorganic filler such as carbon nanotubes (CNTs) to produce mixed matrix membrane (MMM).

Acknowledgments

The authors would like to appreciate Ministry of Higher Education Malaysia (MOHE) for providing Fundamental Research Grant Scheme (FRGS) (MOHE Ref. No: FRGS/1/2015/TK02/CURTIN/03/1) and Cost Centre: 001048. Also, the authors would also like to thank LRGS USM (Account No: 304/PJKIMIA/6050296/U124), and Curtin Cost Centre: 001047.

References

[1.] Zhang Y et al 2013 *Int. J. of Greenhouse Gas Control*. **12** p 84-107
[2.] Zhang W et al 2008 *Chem. Ind. and Engr. Progr*. **27**(5) p 635
[3.] Nyambura M G et al 2011 *J. of Env. Mgmt*. **92**(3) p 655-64
[4.] Pan S Y, E Chang and P C Chiang 2012 *Aerosol Air Qual Res*. **12**(5) p 770-91
[5.] Zhang Z E et al 2014 *Glob. Nest J*. **16** p 355-74

[6.] Dortmundt D and K Doshi 1999 UOP LLC.
[7.] Kohl A L and R Nielsen 1997 *Gulf Prof Publishing*.
[8.] Ismail A F et al 2009 *Separ. and P. Tech*. **70**(1) p 12-26
[9.] Paradise M and T Goswami 2007 *M & Design*. **28**(5) p 1477-89
[10.] Low B T et al 2013 *J. of Mem. Science*. **431** p 139-55
[11.] Baker R W 2002 *Ind. & Engr. Chem. Research*. **41**(6) p 1393-411
[12.] Basu S et al 2010 *Chem. So.c Reviews*. **39**(2) p 750-68
[13.] Kunthadong P et al 2015 *J. of Polymers and the Env*. **23**(1) p 107-13
[14.] Jansen J C et al 2005 *Polymer*. **46**(25) p 11366-79
[15.] Kesting R E and A Fritzsche 1993 *Wiley-Interscience.*
[16.] Paulsen F G, S S Shojaie and W B Krantz 1994 *J. of Mem. Science*. **91**(3) p 265-82
[17.] Jansen J C et al 2006 *J. of Mem. Science*. **272**(1) p 188-97
[18.] Xie S M et al 2008 *J. of Mem. Science*. **321**(2) p 293-8
[19.] Feng Y, J M Zhang and J Zhang 2015 *ACTA POLYMERICA SINICA*. **12** p 1396-401
[20.] S.Minhas B 1992 *Google Patents*.
[21.] Sadeghi M, M A Semsarzadeh and H Moadel 2009 *J. of Mem. Science*. **331**(1) p 21-30
[22.] Ismail A F et al 2011 *Separ. and P. Tech*. **80**(1) p 20-31
[23.] Baker R W, J Wijmans and Y Huang 2010 *J. of Mem. Science*. **348**(1) p 346-52
[24.] Ong A L et al 2008 *J. of Power Sources*. **183**(1) p 62-8
[25.] Oyama K O N, E L Siqueira and M d Santos 2002 *Brazilian dental J.* **13**(3) p 208-11
[26.] Xing D Y, N Peng and T S Chung 2010 *Ind. & Engr Chem. Research*. **49**(18) p 8761-9
[27.] Yang Y Y, T S Chung and N. Ping Ng 2001 *Biomaterials*. **22**(3) p 231-41
[28.] Mao Y et al 2006 *J. of Mem. Science*. **279**(1–2) p 246-55
[29.] N Widjojo, TS Chung, S Kulprathipanja 2008 *J. of Mem. Science.* **25**(1) p 326-35